

Diffusion-Weighted and Fluid-Attenuated Inversion Recovery Imaging in Creutzfeldt-Jakob Disease: High Sensitivity and Specificity for Diagnosis

Geoffrey S. Young, Michael D. Geschwind, Nancy J. Fischbein, Jennifer L. Martindale, Roland G. Henry, Songling Liu, Ying Lu, Stephen Wong, Hong Liu, Bruce L. Miller, and William P. Dillon

BACKGROUND AND PURPOSE: Abnormalities on diffusion-weighted images (DWIs) and fluid-attenuated inversion recovery (FLAIR) images are reported in Creutzfeldt-Jakob disease (CJD). To our knowledge, no large study has been conducted to determine the sensitivity and specificity of DWI and FLAIR imaging for diagnosing CJD.

METHODS: Two neuroradiologists, blinded to diagnosis, retrospectively evaluated DWI and FLAIR images from 40 patients with probable or definite CJD and 53 control subjects with other forms of dementia and rated the likelihood of CJD on the basis of the imaging findings.

RESULTS: DWI and FLAIR imaging was 91% sensitive, 95% specific, and 94% accurate for CJD. Interrater reliability was high ($\kappa = 0.93$). Sensitivity was higher for DWI than FLAIR imaging. Abnormalities involved cortex and deep gray matter (striatum and/or thalamus) in 68% of patients with CJD, cortex alone in 24%, and deep gray matter alone in 5%. The most typical and specific patterns were corresponding hyperintensity on both FLAIR images and DWIs confined to the gray matter in the cortex, striatum, medial and/or posterior thalamus, or a combination of these areas. Narrow-window soft-copy review of artifact-free DWIs and FLAIR images and recognition of the normal variation in cortical signal intensity proved critical for successful differentiation of CJD from other dementias.

CONCLUSION: Because specific patterns of abnormality on DWI and FLAIR images are highly sensitive and specific for CJD, these sequences should be performed whenever CJD is suspected.

Creutzfeldt-Jakob disease (CJD) is a rapidly progressive, fatal neurodegenerative disease caused by accumulation of an abnormally shaped membrane-bound

protein, the prion protein, in neurons (1). In the 85% of cases classified as sporadic CJD (sCJD), no etiology can be identified. Genetic cases, or familial CJD (fCJD), account for 15%; infectious or iatrogenic cases, including variant CJD (vCJD) and iatrogenic CJD, comprise less than 1% (1).

Although motor, cerebellar, visual, and behavioral/psychiatric symptoms are typical of CJD, these symptoms also often occur in other degenerative, infectious, autoimmune or neoplastic diseases of the CNS (2). Current diagnostic criteria for probable sCJD require a combination of specific neurologic symptoms in addition to a characteristic EEG, with 1-Hz periodic epileptiform discharges, or the demonstration of the 14-3-3 protein in the CSF. Cases without the typical EEG or the 14-3-3 protein are considered possible CJD. Definite CJD requires pathologic confirmation on brain biopsy or autopsy (3). Unfortunately, the EEG is often characteristic only late in the course of CJD, has variable sensitivity of 65–85%,

Received September 6, 2004; accepted after revision December 16.

From the Departments of Radiology (G.S.Y., N.J.F., R.G.H., S.L., Y.L., S.W., H.L., W.P.D.), and Neurology (M.D.G., J.L.M., B.L.M.), University of California, San Francisco.

Supported by the John Douglas French Foundation for Alzheimer's Research, the McBean Family Foundation, National Institute on Aging (NIA) grant AG10129, NIA grant P50-AG05142, NIA grant AG16570, NIA K23 AG021989-01, National Institutes of Health Contract NS02328, Alzheimer's Disease Research Centers, the State of California, Alzheimer's Disease Research Center of California, grant 01-154-20 and the National Center for Research Resources, General Clinical Research Center grant M01 RR-00079, U.S. Public Health Service.

G.S.Y. and M.D.G. contributed equally to this work.

Address reprint requests to William P. Dillon, MD, P.O. Box 0628, University of California, San Francisco, San Francisco, CA 74143-0628.

and is not always specific (4, 5). CSF 14-3-3 protein is a controversial marker for CJD, with wide ranges of sensitivity of 53–100% and specificity of 84–100% (5, 6).

Early MR imaging studies revealed normal diffuse cortical atrophy late in CJD (7, 8). Subsequent reports documented T2 prolongation in the basal ganglia, thalamus, cortex (cortical ribboning), or a combination of these areas (9–13). Symmetric hyperintensities in the basal ganglia on T2- and proton density-weighted images have a reported sensitivity of 79% (11). The advent of fluid-attenuated inversion recovery (FLAIR) imaging and, later, diffusion-weighted imaging (DWI) added sensitivity to standard T2-weighted imaging, particularly for the detection of cortical ribboning (9, 14–18).

Although results of a preliminary assessment with DWI and FLAIR imaging in definite CJD suggested high sensitivity (19), few blinded studies have been done to evaluate its utility in diagnosis. The largest study to date revealed a sensitivity of 67% and a specificity of 93% for hyperintensity in the basal ganglia on T2-weighted and FLAIR images; however, investigators obtained DWIs in only five of 162 patients with CJD (all with positive findings), and they did not report interrater reliability (20). Shiga et al (21) reported 92% sensitivity and 94% specificity with hard-copy DWI; the sensitivity of DWI for CJD was far superior to that of FLAIR or T2-weighted imaging. However, they did not examine specificity of FLAIR and T2-weighted images, and their method for assessing specificity was questionable. Despite these reports and the increasing use of MR imaging for the clinical diagnosis of CJD, it has not been incorporated into formal diagnostic criteria.

The goal of this study was to assess the sensitivity and specificity of both hard- and soft-copy DWI and FLAIR imaging in the differentiation of CJD from other nonprion dementias by using criteria based on published reports and our experience with MR imaging-based diagnosis of CJD.

Methods

Patients and Control Subjects

Approval for this study was obtained from the Committee on Human Research at our institution. DWIs and FLAIR images were obtained in 40 patients with sCJD or fCJD and in 53 control subjects with nonprion dementias. All had been referred to our dementia clinic for evaluation between July 2001 and November 2002. The CJD group included 23 patients with definite sCJD (22), 11 with probable sCJD, and six with fCJD (four with *E200K* mutations, one fCJD with an octapeptide repeat, and one Gerstmann-Sträussler-Scheinker syndrome). The 11 patients with probable sCJD fulfilled the Masters probable criteria for CJD (23) and the World Health Organization possible criteria for CJD (3), and eight met the World Health Organization probable CJD criteria (3).

The control group included the following: 11 patients with Alzheimer disease; nine with mild cognitive impairment; seven with frontotemporal dementia; four with dementia with Lewy bodies; four with mixed Alzheimer disease and vascular dementia; three with corticobasal degeneration; three with rapidly progressive encephalopathy (all recovered); two with en-

cephalitis (both recovered); two with memory complaints; and one each with progressive supranuclear palsy, leukoencephalopathy, bipolar disorder, hypoxia, multiple system atrophy, paroxysmal dystonia, vascular dementia, and paraneoplastic cerebellar degeneration (anti-Yo antibody).

Image Review Groups

Although some patients with CJD and control subjects underwent several MR examinations, we included only the earliest studies in our analysis. Because images from many outside institutions were available only on film, we divided the overall cohort into two groups based on image display technique: In one group (digital), images in 12 patients with CJD and 28 control subjects were reviewed on a digital display system that allowed the reader to dynamically adjust the window and level, and in the other group (film), images in 28 patients with CJD and 25 control subjects were reviewed on film. Images in the two groups were analyzed separately to detect differences in sensitivity and specificity related to image-display technique.

MR Imaging Protocol

Nine patients with CJD (23%) and 28 control subjects (53%) underwent imaging at our institution. All images acquired by using 1.5-T clinical MR systems (General Electric Medical Systems, Milwaukee, WI) with fast gradients of >20 mT/m and-echo planar capability by using quadrature head coils. We used our standard diagnostic protocol for dementia and standard acquisition parameters, as follows: sagittal T1-weighted spin-echo (TR/TE/NEX = 600/minimal/2), axial and/or coronal FLAIR (TR/TE/TI/NEX = 10000/140/2200/1), and axial and/or coronal three-direction echo-planar DWI (TR/TE/NEX = 8000/minimal/1, *b* factor = 1000 s/mm²). Both coronal and axial FLAIR imaging and DWI were performed in most subjects, and axial DWI and FLAIR imaging were performed in all.

We reviewed only standard sagittal T1-weighted images and axial and/or coronal FLAIR images and DWIs. Because apparent diffusion coefficient maps were not available for most studies performed at outside institutions, we did not evaluate these maps. No phased-array head coils were used in the studies performed at our institution. Because no such coils were commercially available when most of the study data were acquired, it was unlikely that any of outside institutions used these coils. Three outside studies might have been performed at 1.0 T. Use of general anesthesia was necessary in a few patients with CJD because of involuntary movements. Efforts were made to obtain FLAIR images with the subject breathing room air to prevent artifacts due to supplemental oxygenation (24).

MR imaging Data Presentation

DICOM data for the digital group were transferred into to a data warehouse for clinical brain imaging research. The data were then merged with DICOM data for three patients with CJD whose data were acquired elsewhere, de-identified, and randomized (25). The resulting combined dataset was presented on a video monitor by using commercially available DICOM viewing software (eFilm Medical, Toronto, Canada) that allowed the reader full control of the window and level during interpretation. In the digital and film groups, images for patients and control subjects were presented intermixed and in random order.

Readers

Two neuroradiologists (W.P.D., N.J.F.) blinded to clinical data independently reviewed the images for the digital and film groups. The readers applied the criteria to all images and rated

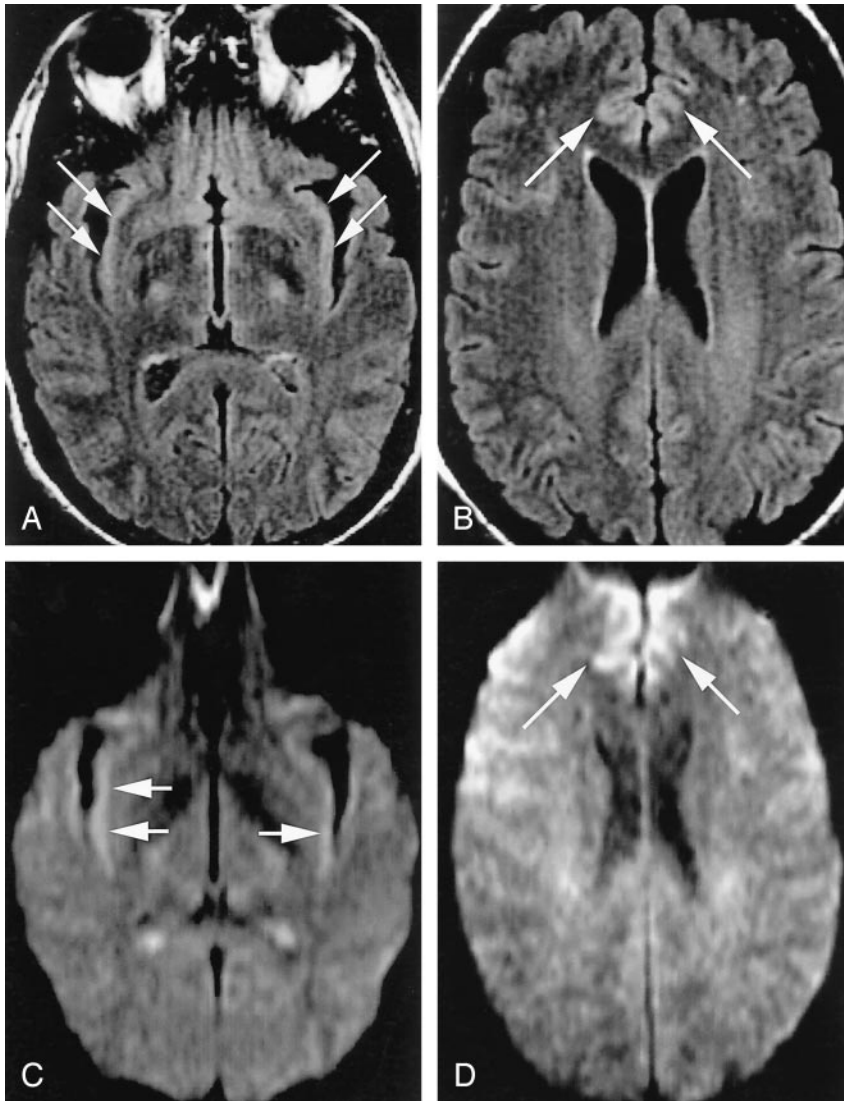


FIG 1. Normal variations, which can complicate assessment of pathologic cortical hyperintensity on FLAIR and DWI.

A, Axial FLAIR (TR/TE/TI = 10000/140/2200) image shows insular cortex slightly hyperintense (arrows) to neocortex.

B, More superior axial FLAIR image shows relative hyperintensity in cingulate cortex (arrows).

C, Axial DWI (TR/TE = 8000/minimal, $b = 1000 \text{ s/mm}^2$, same level as A) shows hyperintensity in bilateral insular cortex (arrows).

D, More superior DWI (same level as B) shows relative hyperintensity cingulate cortex (arrows), accentuated by frontal magnetic susceptibility artifact.

the likelihood that each image represented CJD. Readers also separately noted anatomic areas of abnormality on images obtained with each sequence. Several months later, one of the readers performed a second blinded review of a randomly chosen subset of CJD and control images from the film group to assess intrareader reproducibility. No feedback was given to either reader until all reviews were completed. All images were read twice, once by each reader, with the exception of images in one patient with CJD, whose were read by only one reader. A total of 185 readings was done.

Conventions

Before assigning each subject to an overall diagnostic category, the readers visually graded the signal intensity on DWIs and FLAIR images as normal or abnormal in each of the following anatomic regions: white matter; hippocampus; cingulate gyrus; insula; cortex of the frontal, temporal, parietal, and occipital lobes (including primary visual cortex); precentral and postcentral gyri; striatum (putamen and caudate nuclei); globus pallidus; posterior thalamus; medial thalamus brainstem; middle cerebellar peduncle; and cerebellar cortex. An anatomic region was deemed abnormal when its signal intensity appeared higher than that expected for the same area in a healthy patient, after accounting for normal variations in signal intensity DWI and FLAIR imaging (Fig 1) (26). No quantitative

measurements of signal intensity were obtained because many studies were available only on film and because pathologic cortical thinning created problems with partial-volume averaging in the digital group. The discrete anatomic areas of focal abnormal T2 prolongation and reduced diffusion detected in gray matter were grouped into the following four broad anatomic distributions: 1) limbic and paralimbic cortex, including cingulate, insula, and hippocampus; 2) neocortex, including frontal, parietal, temporal, and occipital areas; 3) striatum, including caudate and putamen; and 4) thalamus. The frequency of involvement of these anatomic locations was compared among all CJD groups, CJD subgroups, and the control group.

Diagnostic Categories

After reviewing each study, the reader assigned the patient's condition to one of four categories: definitely CJD, probably CJD, probably not CJD, or definitely not CJD.

Definitely CJD was diagnosed when a reader noted one of two patterns on DWIs and FLAIR images or on DWIs alone: 1) abnormal unilateral or bilateral high signal intensity involving the striatum AND more than one gyrus of the cerebral cortex involved in ribbon-like fashion without corresponding T1 shortening or 2) extensive cortical ribboning (more than

three gyri) without involvement of underlying the white matter and without evidence of T1 shortening in the same region.

Probably CJD was diagnosed if 1) the criteria for definitely CJD were observed only on FLAIR images without corresponding definite abnormality on DWIs; 2) an abnormality was noted on both FLAIR images and DWIs in a small region that was not extensive enough for definitive diagnosis (e.g., in the cortex of only one or two gyri or in a unilateral focal area of the striatum including the caudate and adjacent anterior putamen); or 3) bilateral striatal and/or bilateral thalamic hyperintensity on DWI and FLAIR images restricted to the medial and posterior thalamus in the absence of cortical abnormality.

Probably not CJD was assigned when 1) the only areas of possible abnormal signal intensity in gray matter were subtle and symmetric in areas of cortex that normally has higher signal intensity in DWI and FLAIR images (insula, cingulum) or 2) potentially abnormal findings were most likely to represent artifact.

Definitely not CJD was diagnosed if 1) the image was normal or 2) the findings were not normal but abnormalities were not consistent with the spectrum of findings described for CJD.

Statistical Analysis

Overall sensitivity and specificity for CJD were evaluated by using the generalized estimation equation to correct for the correlation of evaluations in the same patients (27). Because variation in MR acquisition and display technique was minimal in the digital group but wide in the film group, we separately analyzed the data for each group and for both groups combined. In addition, sensitivity, specificity, and intrareader and interreader variability were separately assessed for the four MR diagnoses.

Analysis of interreader variation was performed between the readers for both the film and digital groups. Because interreader variability for the digital cohort was 0, we decided to forego assessment of intrareader variability for this group and assessed intrareader variability in only the film group. Both intrareader and interreader agreement were characterized as κ statistics on a scale from -1.0 (perfect disagreement) to 1.0 (perfect agreement), where 0.0 indicated agreement no better than expected by chance and values greater than 0.8 represented the highest level of agreement (28). Because authors describe this level of agreement with different terms (e.g., "very good," "excellent," etc) and because the thresholds for these terms are somewhat arbitrary, we directly reported the values by using 95% confidence intervals.

The nonparametric Wilcoxon test was used to compare differences in age and symptom duration between groups and CJD subtypes. The Fisher exact test was used to evaluate associations between disease duration and patterns of abnormality. Diagnostic results were tabulated according to reader and disease type (including CJD subtypes and control diagnoses). Statistical analysis was performed using software (SAS version 8.2; SAS Institute, Cary, NC). A significance level of $P < .05$ was used for all analyses.

After all blinded review sessions were completed, the neuroradiologists reviewed the false-positive and false-negative cases and assigned a probable explanation for each diagnostic error by consensus.

Patient Subgroup Analyses

Subgroup analyses included an evaluation of the differences between the sCJD and fCJD cohorts to detect heterogeneity in the combined cohort, which might result in underestimation of diagnostic utility, as well as an analysis of the duration of symptoms versus pattern of abnormality. The latter was performed by grouping 38 patients with CJD into groups based on the neurologists' estimate of the duration of symptoms at the time of first MR imaging: early (0–2.9 months, $n = 13$), intermediate (3–6 months, $n = 10$), and late (>6 months, $n = 15$).

TABLE 1: Sensitivity, specificity, and accuracy of FLAIR and DWI in CJD

Image Display	Sensitivity	Specificity	Accuracy
Film	0.88	0.98	0.93
Digital	1.00	0.93	0.95
Combined	0.91	0.95	0.94

Note.—Data based on all readings from both readers.

TABLE 2: Intrareader and interreader concordance in interpreting MR images

Image Display	Intrareader*	Interreader		
		Film	Digital	Combined
Observed agreement	0.93	0.92	1.00	0.96
Predicted chance agreement	0.53	0.50	0.56	0.51
κ	0.86	0.85	1.00	0.91

* Film only. Digital not included because of 100% interreader agreement.

Two patients were excluded from this analysis because their duration of symptoms was uncertain.

Subgroup Analyses

The film and digital groups were compared. Because previous investigators have demonstrated that DWI significantly increases sensitivity in detecting CJD compared with FLAIR imaging, alone we did not readdress this issue by reading FLAIR images and DWIs separately (16, 29).

Results

Group Characteristics

The control group was older than the patients with CJD (mean, 67 vs 58 years; $P = .0003$, Wilcoxon test) and had a longer duration of symptoms at the time of MR imaging (41 vs 12 months; $P < .0001$, Wilcoxon test).

Diagnostic Utility of DWI and FLAIR Imaging

Table 1 presents the sensitivity, specificity and accuracy of combined FLAIR and DWI images. Overall sensitivity for the diagnosis of CJD was 91%, specificity was 95%, and accuracy was 94%. Interreader concordance was high in the film group ($\kappa = 0.85$) and complete ($\kappa = 1.00$) in the digital group. Hence, unless otherwise stated, our results refer to the total readings of the two readers. Intrareader concordance for film review was also high ($\kappa = 0.86$) (Table 2).

Regional assessment of abnormality on FLAIR images, DWIs, or both was performed for multiple areas of cortex and deep gray matter. Abnormality was observed on both images in 83% of patients with CJD and in 8% of control subjects. Therefore, the presence of abnormality on images obtained with both sequences was strongly predictive of CJD (84% sensitivity and 91% specificity). Abnormality on DWIs or FLAIR images alone was seen in 4% of patients with CJD and 4% of control subjects. Therefore, the ob-

TABLE 3: Percentages of cases with gray matter abnormalities

Region	CJD (n = 40)	Control (n = 53)
Neocortex	89	17
Frontal	84	9
Rolandic	0	1
Parietal	72	3
Temporal	65	11
Primary visual	9	1
Occipital	39	2
Limbic	79	25
Striatum	69	4
Thalamus	34	0
Neocortex and striatum	68	0
Neocortex without striatum	24	11
Striatum without neocortex	5	2
Limbic alone	0	13
No abnormality	5	68

ervation of abnormality on one of the two images was neither sensitive nor specific.

Table 3 shows the patterns of gray matter abnormalities observed on FLAIR and DWI combined. Abnormal hyperintensity in the neocortex (Fig 2) and limbic cortex, respectively, was seen in 89% and 79% of patients with CJD and in 17% and 25% of control subjects. In no patient with CJD was the signal intensity of the central sulcus or precentral gyrus abnormal despite the finding of neocortical signal intensity abnormality in adjacent posterior frontal and/or anterior parietal gyri (Fig 3). Primary visual cortex was also relatively spared (Fig 2), having been judged abnormal in 9% of those with CJD.

Abnormal signal intensity in the striatum was seen less frequently than neocortical involvement in patients with CJD (69% vs 89%) and rarely in control subjects (4%). In 68% of patients with CJD, both neocortical and striatal abnormality was present (Fig 4). In patients with CJD, images showed abnormal signal intensity in neocortex but not striatum in 24% (Fig 2) and signal intensity abnormality in deep gray matter (primarily striatum) but not neocortex in approximately 5% (Fig 5). We found a predilection for involvement of the anterior aspect of the putamen over the posterior, as well as for the head of the caudate nucleus over the body (Fig 6).

Abnormal thalamic signal intensity was seen in 34% of patients with CJD and no control subject (Fig 7). The abnormal signal intensity involved the medial or posterior aspect of the thalamus in all patients but one, in whom images showed subtle diffuse involvement (discussed later). In no case was isolated abnormality observed. Unilateral frontal or parietal neocortical involvement was frequently associated with ipsilateral thalamic involvement and less commonly associated with contralateral thalamic abnormality. No significant lesions were observed in the cerebellum, brainstem, or globus pallidus. Although abnormal signal intensity in the white matter and volume loss were both slightly more widespread and severe in the control group (64% and 69%, respectively) than

the CJD groups (49% and 60%, respectively), the differences were not significant.

Degree of Perceived Diagnostic Certainty

We performed 185 readings (imaging diagnoses). Of the 155 definite diagnoses (subset of readings by the two readers in the 93 subjects classified as either definitely CJD or definitely not CJD), no false-positive and five false-negative results occurred (Table 4). Of the 30 diagnoses of probably CJD or probably not CJD, five false-positive and two false-negative results occurred (Table 4). This yielded 93% sensitivity and 100% specificity for definite diagnoses considered alone and 83% sensitivity and 72% specificity for probable diagnoses considered alone.

False-Positive and False-Negative Results

Findings in three control subjects were misdiagnosed as those of CJD, by both readers in two, producing five false-positive readings. Consensus review of three false-positive diagnoses in two cases (one by both readers in the digital group and one by a single reader in the film group) revealed the abnormality on the FLAIR image alone (isolated FLAIR abnormality). One patient had frontotemporal dementia and the other had memory complaints. Consensus re-review indicated that the FLAIR images of the patient with frontotemporal dementia were abnormal but the DWIs were not. In both patients, the abnormality on FLAIR was thought to involve limbic cortex and neocortex but not striatum. Isolated FLAIR abnormality, as seen in these patients, was noted in 4% of patients with CJD and 3% of control subjects. Consensus review of the third false-positive case (digital group), which both readers called probably CJD, showed that abnormal signal intensity involved limbic cortex with only subtle accompanying hyperintensity in the thalami (Fig 8). On physical examination, this patient had severe dystonia, which later resolved, raising the possibility that another underlying process affected the striatum. Abnormality restricted to limbic cortex was noted in seven control subjects (13%) but in no patient with CJD.

Between the two readers, five cases of CJD (all in the film group), including two cases of fCJD, were misdiagnosed as not CJD. Both readers misinterpreted two of these cases, producing seven false-negative diagnoses. Consensus review showed subtle findings in four of the five cases, particularly on DWI. Re-review of one false-negative case revealed that the abnormality was primarily restricted to the striatum and thalamus (Fig 9) and that it was more diffuse than the typical sharply localized posterior and medial thalamic findings seen in other cases of CJD. In three cases (including two of fCJD), severe magnetic susceptibility, patient motion artifacts, or poor selection of display window during filming (Fig 10) compromised the interpretation. The plane of section per se (axial or coronal), independent of artifacts, windowing, signal-to-noise ratio, and contrast-to-noise ratio, were not thought to substantially contribute to

FIG 2. A 50-year-old man with definite sCJD.

A, Axial DWI shows pathologic hyperintensity in bilateral posterior temporoparietal neocortex. Cortex along parieto-occipital fissure is abnormally hyperintense (vertical arrows), but primary visual region is spared (horizontal arrows). Note asymmetric abnormal hyperintensity in right cingulum (arrowhead). Striatum is uninvolved.

B, FLAIR image at same level shows more subtle pathologic hyperintensity in all abnormal regions on DWI, as shown in cingulate cortex (arrowhead).

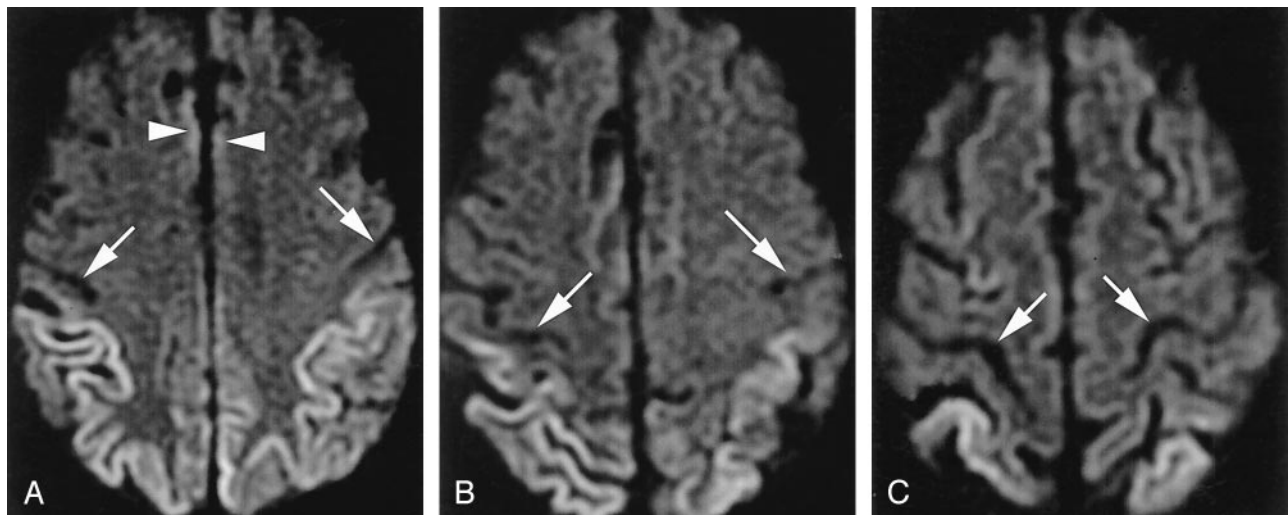
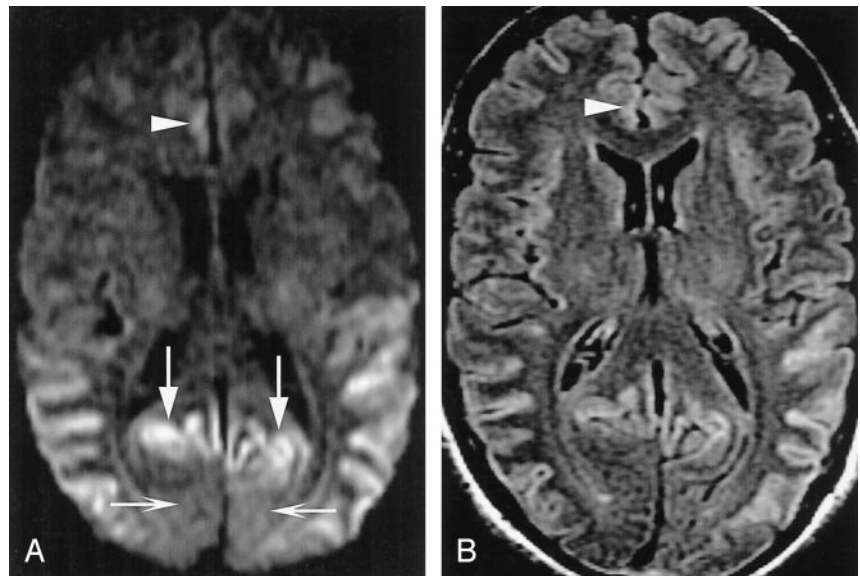


FIG 3. A 52-year-old man with probable sCJD.

A, Axial DWI shows pathologic hyperintensity in bilateral parietal neocortex and sparing of cortex in postcentral gyrus along the central sulcus (arrows) and entire precentral gyrus. Note subtle abnormality of paramedian frontal cortex (arrowheads).

B, More superior DWI shows relatively sparing of cortex on both sides of central sulcus (arrows).

C, More superior DWI confirms identification of central sulcus (arrows) and sparing of precentral and postcentral gyri.

the false-negative diagnoses. Many of our standard protocols include both axial and coronal FLAIR imaging and DWI; therefore, the reviewers were thoroughly familiar with the different artifacts (including susceptibility and flow artifacts), and normal appearance of cortical signal intensity variation on coronal and axial DWI and FLAIR imaging.

Imaging Results Across Subgroups

We found no significant difference in symptom duration at the time of imaging in patients with CJD, as analyzed by display group, certainty of diagnosis (probable vs definite), or by CJD subtype (sCJD vs fCJD). Subgroup analysis revealed no correlation between duration of symptoms and pattern of abnormality. All patterns of abnormality occurred with

roughly equal frequencies among the three (temporally divided) CJD groups. We found a trend toward younger age ($P = .14$, Wilcoxon test) and longer duration of symptoms ($P = .1$, Wilcoxon test) in the fCJD group compared with the sCJD group. Frequency or anatomic distribution of gray matter abnormality did not obviously differ between the groups.

Discussion

Case and study reports have suggested that specific brain regions are abnormal on MR imaging in CJD. The goal of our study was to examine the utility of MR imaging with both DWI and FLAIR imaging in the diagnosis of CJD. Using MR criteria, we found 91% sensitivity, 95% specificity, and 94% accuracy in differentiating CJD from other dementias, with high

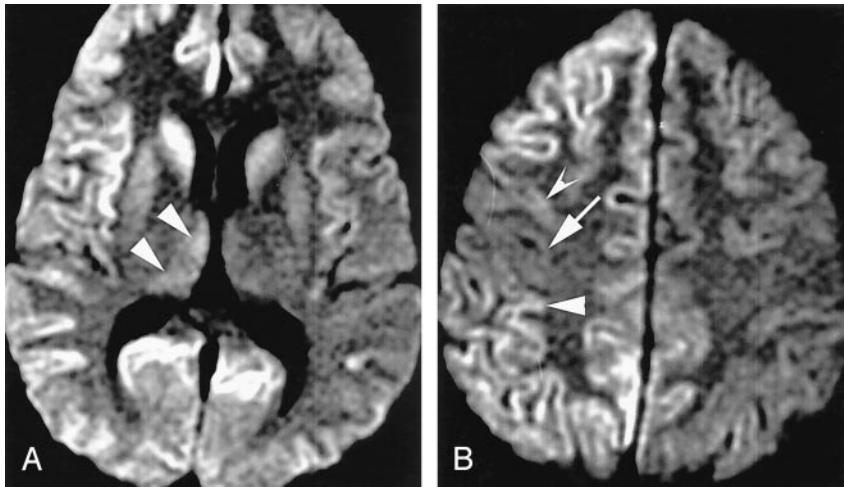


FIG 4. A 26-year-old man with sCJD. A, Axial DWI shows extensive, asymmetric, right-greater-than-left neocortical involvement and abnormal hyperintensity of right caudate nucleus, putamen, and thalamus (arrowheads). Left caudate nucleus may be mildly hyperintense, but left putamen and thalamus are not definitely abnormal.

B, More superior axial DWI shows involvement of posterior frontal (top arrowhead) and anterior parietal (bottom arrowhead) cortex, with sparing of cortex on edges of the central sulcus (arrow).

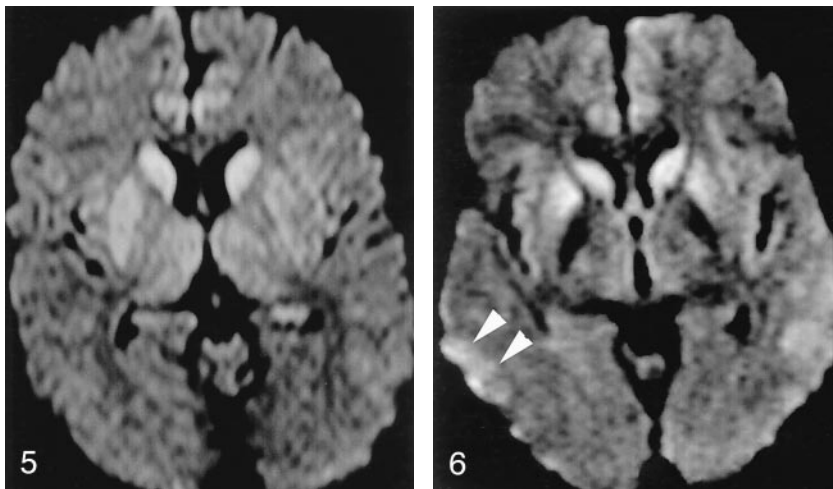


FIG 5. Striatum without neocortical involvement. Axial DWI in a 40-year-old man with sCJD shows abnormal symmetric hyperintensity in bilateral caudate nuclei, right putamen, and possibly right thalamus. Left putamen and thalamus are not definitely abnormal. Mild hyperintensity in bilateral cingulate cortex is thought to be normal variation and magnetic susceptibility artifact.

FIG 6. Axial DWI in a 78-year-old woman with sCJD shows symmetric hyperintensity in bilateral caudate nuclei and anterior putamina. No definite neocortical involvement is seen, as temporal hyperintensity (arrowheads) is thought to be magnetic susceptibility artifact, and appearance of insular and cingulate cortices may be within normal limits.

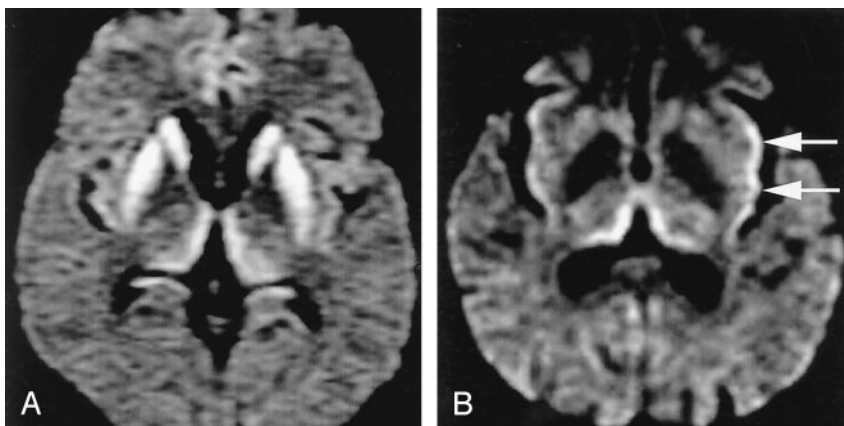


FIG 7. Abnormal thalamic appearance in sCJD.

A, DWI in a 41-year-old man shows symmetric hyperintensity in bilateral caudate nuclei and putamina and medial and posterior thalami (double hockey stick). No definite neocortical abnormality is seen. Cingulate cortex and insular cortices are mildly hyperintense but likely within normal limits.

B, Axial DWI in a 59-year-old woman shows abnormal hyperintensity in bilateral medial thalami and pulvinar. Left insular cortex (arrows) was thought to be definitely abnormal, and right, possibly abnormal. Caudate nuclei and putamina are spared.

intrarater and interrater reliability. Increased sensitivity (93%) and specificity (100%) was achieved in diagnosing cases that met definite radiologic criteria, and slightly decreased sensitivity (83%) and specificity (72%) was achieved in the diagnostic group meeting only probable criteria. Because the relatively small number of probable diagnoses made the sensitivity and specificity estimates for this subgroup less reliable than they would have been otherwise, the sensitivity and specificity calculated for the aggregate

of all cases likely remains the most informative and reliable measure of diagnostic utility to emerge from our study.

Extensive abnormal hyperintensity in cortical gray matter on both FLAIR images and DWIs, particularly with accompanying striatal abnormality with or without thalamic abnormality, strongly suggested CJD. Abnormality appreciated only FLAIR images and not DWIs was atypical for CJD and may suggest an alternative diagnosis.

TABLE 4: Diagnostic utility analysis by degree of radiologic diagnostic certainty

Result	Definite Diagnoses* (n = 155)	Probable Diagnoses† (n = 30)
Group		
Not CJD	88/0	13/5
CJD	5/62	2/10
Utility		
Sensitivity	0.93	0.83
Specificity	1.00	0.72

Note.—No. of diagnoses are negative/positive findings on MR imaging.

* Read as “definitely CJD” or “definitely not CJD.”

† Read as “probably CJD” or “probably not CJD.”

Previous Literature

The literature on brain MR imaging in CJD, largely comprising single case reports and small case series since the late 1980s, may be divided as follows: initial reports before the use of FLAIR imaging showing low sensitivity of routine MR imaging sequences for CJD (11, 30), reports of significantly improved sensitivity for CJD with the introduction of FLAIR sequences (18, 31, 32), and several reports suggesting that DWI improves the sensitivity of MR imaging for CJD (13, 15–17, 33, 34).

Although the literature established the constellation of MR findings characteristic of CJD, the sensitivity and specificity of DWI and FLAIR sequences for CJD had not been established, nor had film versus digital viewing been compared, to our knowledge. This information is needed for MR imaging, with DWI and FLAIR imaging, to be incorporated into clinical diagnostic algorithms. Such improved algorithms may help reduce costs, lower patient morbidity rates, and reduce risks to patients and hospital staff by obviating surgical biopsy.

In a retrospective blinded review of 162 patients and 58 control subjects, the sensitivity of bilateral, symmetric hyperintensities in the basal ganglia on T2-weighted images was 67%, and the specificity at 93%, but DWI and FLAIR imaging were not routinely used. As the authors acknowledged, this limitation and heterogeneity of their MR techniques mean that this sensitivity is likely an underestimate (20). Another study demonstrated the superiority of DWI to FLAIR imaging alone in 13 patients with CJD (definite and probable sCJD and fCJD) and, by extension to MR imaging without DWI or FLAIR imaging (16). However, because control group was included, the specificity could not be estimated. In this study, all patients had striatal and/or cerebral cortical lesions; the thalamus was involved in only one patient. In a retrospective study, Shiga et al found that DWI had higher sensitivity for CJD (92%) than FLAIR imaging (41%–59%), T2-weighted imaging (36%–50%), EEG (50%–78%), or testing for CSF protein 14-3-3 (84%) or neuron specific enolase (73%). Among 26 patients with CJD and 32 control subjects with dementia, DWI had specificity of about 94% for CJD. Only film images were used, and they

did not examine the specificity of combination of DWI and FLAIR imaging or of FLAIR imaging alone (21). Our report adds to this literature, showing the benefit of digital viewing and the high sensitivity and specificity of combined DWI and FLAIR imaging for CJD.

Patterns of Abnormality

The literature reports that T2 prolongation and reduced diffusion most frequently involve the corpus striatum (10, 35), followed by the neocortex (10, 13, 16, 17), and the posterior and medial thalamus (11, 16, 17). A small number of reports describe T1 shortening in the globus pallidus (11, 20, 36), and a few case reports note abnormal T2 prolongation in the cingulum (35–37), cerebellum (20, 38), hippocampus (38) and insula (37). Reports from East Asia have documented extensive abnormal signal intensity in the white matter and atrophy in some cases of sCJD (8, 39, 40). Our study showed no significant difference in white matter signal intensity between the sCJD and control groups, suggesting the possibility that a distinct, predominantly East Asian panencephalic subtype of sCJD exists. The few reports of MR findings in fCJD, due to variety of mutations of prion gene, have documented a similar spectrum of findings (16, 21, 41, 42). Although we found no significant differences between our sCJD and fCJD cohorts, differences may begin to emerge in a larger fCJD group. Reports of vCJD describe abnormalities in similar anatomic regions. However, in vCJD, abnormality of the posterior (pulvinar) and medial thalamus is most common; this is followed by abnormality in the periaqueductal gray matter; the striatum; and, less commonly, the neocortex. The pulvinar sign, defined by increased intensity in the pulvinar relative to the anterior putamen, appears to be the most sensitive radiologic marker for vCJD (43, 44).

In our CJD group, gray matter abnormality was most often seen in neocortex (89%), followed by limbic cortex (79%), striatum (69%), and thalamus (34%). In the neocortex, abnormal high signal intensity was most often present in the frontal lobes (84%), followed by the parietal (72%) and temporal (65%) lobes. This distribution seems to roughly parallel the sizes of the lobes, possibly suggesting that any area of cerebral cortex may be involved with nearly equal probability, with the notable exception of primary sensorimotor and visual cortices. In control subjects, increased signal intensity was noted more often in frontal and temporal neocortex than in parietal or occipital neocortex. In retrospect, this seems likely because the inferior frontal pole (adjacent to the planum sphenoidale and frontal sinus) and the inferior temporal lobes (adjacent to the petrous temporal bone and occiput) are the areas of neocortex most affected by susceptibility artifacts on echo-planar imaging such as DWI. Additional information regarding patterns of involvement on MR imaging emerged from our analysis. The three most prevalent patterns of gray

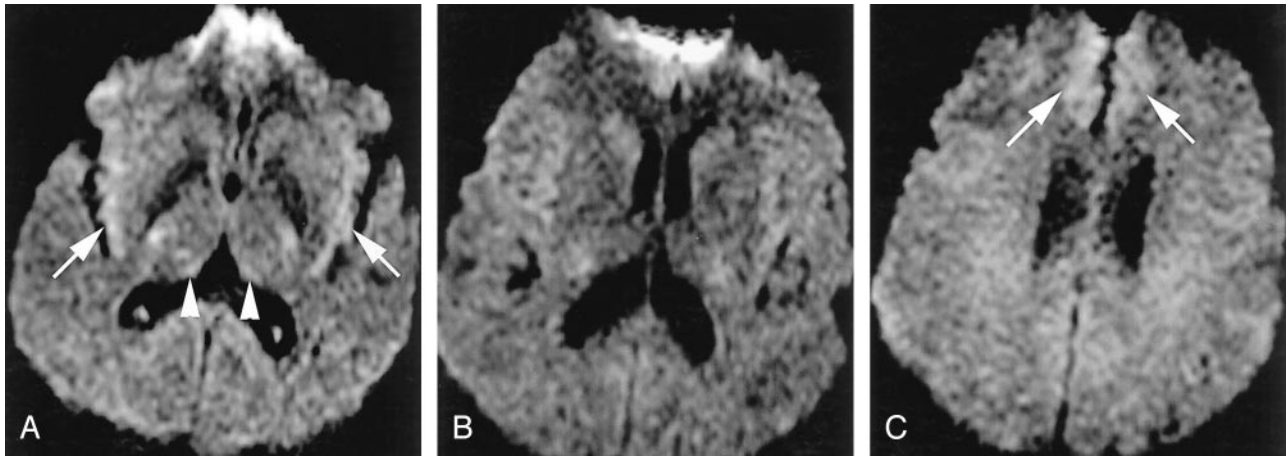


FIG 8. False-positive CJD. Patient had mild cognitive impairment.

A, On DWI, signal intensities of insular cortices (arrows) and dorsomedial thalami (arrowheads) were called abnormal.
 B, More superior DWI shows no clear abnormality, although subtle hyperintensity in caudate nuclei is questioned. Magnetic susceptibility artifact somewhat obscure frontal lobes.
 C, More superior DWI suggests abnormal hyperintensity of medial frontal lobes.

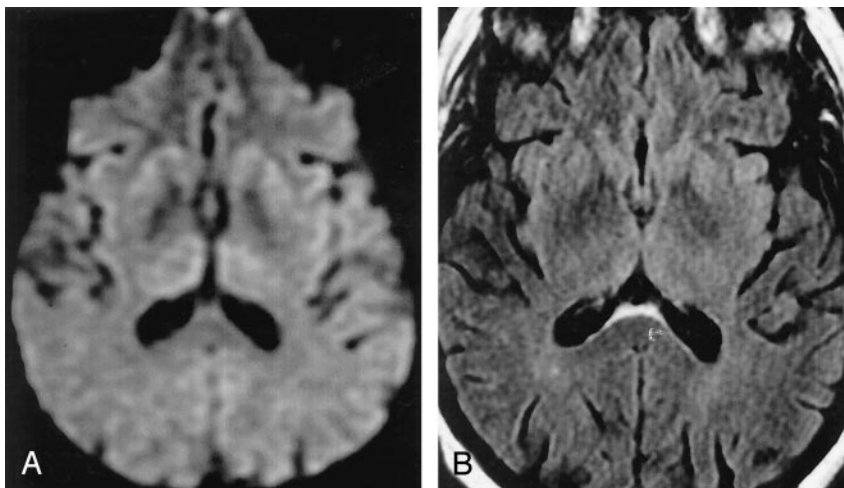


FIG 9. False-negative CJD.

A, Axial DWI (poor windows, film cohort) in a 65-year-old man with definite sCJD retrospectively shows subtle hyperintensity of bilateral caudate heads and anterior putamina. Medial and dorsal thalami are subtly abnormal but more diffusely than is typical of CJD. Insular cortex may be pathologically hyperintense or normal.
 B, Even in retrospect, calling an abnormality on corresponding FLAIR image (mildly motion degraded) is difficult.

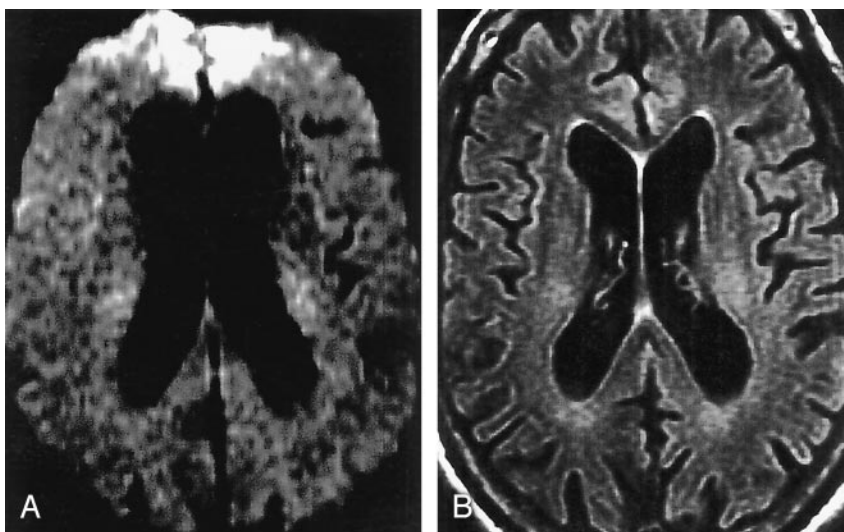


FIG 10. False-negative CJD (film cohort).

A, Axial DWI in a 49-year-old man with definite sCJD shows no clear abnormality. Image is motion degraded and poorly windowed, with severe magnetic susceptibility artifact in bifrontal regions.
 B, Corresponding FLAIR image shows marked prominence of ventricles and sulci for the patient's age. In retrospect, extensive cortical thinning and probably pathologic hyperintensity are found. CJD not called because of lack of DWI confirmation and difficulty in assessing thin cortex in this patient (with clinical signs for >6 months).

matter abnormality, occurring in 76% of our cases of CJD, were limbic cortex and neocortex alone (32%) (Figs 2A, 3A); limbic cortex, neocortex, and

striatum (29%); and limbic cortex, neocortex, striatum, and thalamus (15%) (Fig 4A). Predominant involvement of the anterior striatum with sparing of

the globus pallidus was frequent, either in isolation or in conjunction with neocortical and/or thalamic abnormalities.

Thalamic involvement was primarily limited to medial and posterior thalamus and always associated with striatal and neocortical abnormality. Although this feature may typically help differentiate to sCJD from vCJD, in which the pulvinar sign is frequently present alone, a case of sCJD in which T2-weighted images, FLAIR images, and DWI showed only the pulvinar sign has been reported (45).

Unilateral neocortical hyperintensity ipsilateral to unilateral hyperintensity in the deep gray matter was a frequently observed pattern that should be recognized as typical of CJD, as conditions such as metabolic abnormalities or global anoxic injuries might be expected to be more symmetric. No abnormality in the posterior fossa was identified. Although this finding suggests that the cerebellum is generally spared in the more common clinical variants of CJD, no cases of clinically cerebellar predominant (Brownell-Openheimer) CJD were present in our cohort.

Sparing of Primary Sensorimotor and Visual Cortices

Even in the presence of extensive abnormal signal intensity in the frontal and parietal cortex, the primary motor and sensory cortices on either side of the central sulcus (Rolandic cortex) were never identified as being abnormal in our CJD group (Fig 3 and Table 3). However, after our study was completed, we observed involvement of the cortex of the postcentral gyrus in a patient with clinically definite CJD. This relative sensorimotor sparing mirrors the clinical observation that CJD appears to relatively spare primary somatosensory cortical function. Although primary visual cortex was also relatively spared in our CJD group (involved in 9%), no cases of the Heidenhain (occipital) variant of sCJD were present, a finding that may have influenced the results (46). Variation in the patterns of involvement in specific brain regions is likely related to the underlying pathologic and/or physiologic abnormalities and warrants further study.

Preliminary data in humans suggest that the DWI hyperintensity is best correlated with vacuolation (spongiform change) and, to a lesser extent, with gliosis and neuronal loss (S. J. DeArmond, unpublished data, 2004). On the contrary, increased signal intensity on T2-weighted and DWI in the brains of scrapie-infected mice is most strongly correlated with the deposition of the abnormal prion protein and astrocytic gliosis than with vacuolation (47). Results suggesting that the strain of prion (determined by protein conformation), glycosylation composition, and genetic factors influences the pattern and type of pathologic involvement (48, 49) may explain these differences.

Pitfalls in Diagnosis

During the re-review of our false-negative and false-positive cases, we identified a number of poten-

tially avoidable pitfalls related to image acquisition and display and to normal variations of signal intensity in regions commonly involved in CJD. Susceptibility artifacts may substantially reduce diagnostic accuracy, particularly near the skull base (i.e., inferior frontal and temporal lobes). Motion artifact was problematic in a number of cases, especially in regions of the brain already compromised by susceptibility. The speed of acquisition with DWI sequences can help to reduce motion artifact in patients who cannot remain still for prolonged periods because of myoclonus and/or dementia, but general anesthesia may still be required to obtain diagnostic-quality images. Suboptimal selection of display windows during viewing was responsible for two of five false-negative diagnoses in the film cohort. In four of these cases, the abnormal findings were subtle. However, no false-negative diagnoses were encountered during digital review of images in a similar patient population that also had subtle findings. This observation underscores the considerable advantages of soft-copy display, which allows a reader to adjust window levels for optimal interpretation.

An abnormality that is appreciated only FLAIR images and not DWIs, as occurred in two of our three false-positive cases, should be regarded as atypical for CJD and suggest an alternative diagnosis. For example, the paraneoplastic condition associated with CRMP-5 antibodies clinically overlaps with CJD; this results in high T2 signal intensity on FLAIR images of the basal ganglia but not in the cortex or thalamus, and DWIs have been reported to be normal (50). Collie et al reported a case of vCJD in which pulvinar abnormalities detected on FLAIR images were not identified on DWIs, but they did not note whether digital or film analysis was done (43). Of note, relatively high signal intensity on FLAIR images confined to limbic cortex alone should not suggest CJD, as the signal intensity of these regions is higher than that of adjacent neocortex on normal studies (51). To avoid this pitfall, which was the basis of one of our false-positive cases, clinicians and radiologists must familiarize themselves with the normal appearance of limbic gray matter on narrowly windowed FLAIR images and DWIs (Fig 1).

In clinical practice, imaging findings of CJD are often overlooked, likely because the abnormalities are subtle or misinterpreted as artifact or possibly because their symmetry is sometimes striking. In one study, neuroradiologists or radiologists initially overlooked hyperintensities in the basal ganglia on T2- or proton attenuation-weighted MR images in 80% of patients with CJD (20). This observation underscores our need as neurologists and radiologists to educate ourselves about the subtlety of these findings.

ADC Maps

Because ADC maps were not available in the cases from outside our institution, and therefore not included in the analysis, some of the abnormality seen on DWI might have represented T2 prolongation (T2

shine-through effect) in addition to reduced diffusion. Nevertheless, the use of DWIs alone provided high sensitivity and specificity. Therefore, although prolonged reduction of ADC has been documented in CJD (16, 37), the principle advantage of DWI may be the increased tissue contrast it offers for abnormal signal intensity in the gray matter rather than specific detection of reduced water diffusion; in 83% of our patients with CJD, abnormality was appreciated on FLAIR imaging as well as on DWI. Furthermore, ADC maps can be difficult to interpret, especially in the pathologically thin cortex of a patient with late-stage CJD, because of volume averaging with CSF, motion and susceptibility artifacts, and loss of information during postprocessing. Although that availability of ADC maps might shed light on the pathophysiology of CJD, particularly when serial images are obtained over time, the absence of these maps was not considered a notable limitation in the diagnosis of CJD. Lastly, although no surface-coil images were included in this series (to our knowledge), the increasing use of MR phase-array surface head coils requires a word of caution. Such coils tend to produce relative cortical hyperintensity related to their sensitivity profile; we suspect that this hyperintensity could be confused with findings of CJD.

Conclusion

The combination of FLAIR and DWI techniques had sensitivity, specificity, and accuracy of over 90% in the differentiation of CJD from other dementias with high intrareader and interreader reliability. Therefore, this combination should be considered essential for adequate MR evaluation of sCJD. When electronic image display is available, achievable accuracy may be even higher. Conversely, improper data acquisition and display technique and also susceptibility and motion artifacts may substantially impair diagnosis. Familiarity with the normal variation in cortical signal intensity on DWI and FLAIR and with patterns of gray matter hyperintensity typical of CJD is essential for accurate diagnosis. Confirmation of these findings in a prospective cohort is an appropriate next step to revise the diagnostic algorithm for CJD and to definitively establish the full spectrum of MR findings in human prion disease.

Acknowledgments

The authors would like to thank Dr Howard J. Rosen for his careful review and critique of the manuscript and Dr James E. Caldwell for his assistance in providing anesthesia for a some of the MR imaging studies.

References

- Prusiner SB. Prions. *Proc Natl Acad Sci U S A* 95:1998;13363–13383
- Geschwind MD, Jay C. *Alzheimer's Disease and Other Primary Dementias*. In: *Harrison's Principles of Internal Medicine*. Bird T, ed. McGraw Hill, 2003;2391–2398
- World Health Organization. *Global surveillance, diagnosis, and therapy of human transmissible spongiform encephalopathies: report of a WHO consultation*. In: *Global Surveillance, Diagnosis, and Therapy of Human Transmissible Spongiform Encephalopathies*. Geneva: World Health Organization; 1998:1–29
- Tschampa H. Patients with Alzheimer's disease and dementia with Lewy bodies mistaken for Creutzfeldt-Jakob Disease. *J Neurol Neurosurg Psychiatry* 2001;71:33–39
- Zerr I, Pocchiari M, Collins S, et al. Analysis of EEG and CSF 14-3-3 proteins as aids to the diagnosis of Creutzfeldt-Jakob disease. *Neurology* 2000;55:811–815
- Geschwind MD, Martindale JL, Miller D, et al. Challenging the clinical utility of the 14-3-3 protein for the diagnosis of Sporadic Creutzfeldt-Jakob disease. *Arch Neurol* 2003;60:813–816
- Kovanen J, Erkinjuntti T, Iivanainen M, et al. Cerebral MR and CT imaging in Creutzfeldt-Jakob disease. *J Comput Assist Tomogr* 1985;9:125–128
- Uchino A, Yoshinaga M, Shiokawa O, Hata H, Ohno M. Serial MR imaging in Creutzfeldt-Jakob disease. *Neuroradiology* 1991;33:364–367
- Gertz HJ, Henkes H, Cervos-Navarro J. Creutzfeldt-Jakob disease: correlation of MRI and neuropathologic findings. *Neurology* 1988;38:1481–1482
- Yoon SS, Chan S, Chin S, Lee K, Goodman RR. MRI of Creutzfeldt-Jakob disease: asymmetric high signal intensity of the basal ganglia. *Neurology* 1995;45:1932–1933
- Finkenstaedt M, Szudra A, Zerr I, et al. MR imaging of Creutzfeldt-Jakob disease. *Radiology* 1996;199:793–798
- Urbach H, Klisch J, Wolf HK, Brechtelsbauer D, Gass S, Solymosi L. MRI in sporadic Creutzfeldt-Jakob disease: correlation with clinical and neuropathological data. *Neuroradiology* 1998;40:65–70
- Falcone S, Quencer RM, Bowen B, Bruce JH, Naidich TP. Creutzfeldt-Jakob disease: focal symmetrical cortical involvement demonstrated by MR imaging. *AJNR Am J Neuroradiol* 1992;13:403–406
- Urbach H. Creutzfeldt-Jakob disease: analysis of the MRI signal. *Neuroreport* 2000;11:L5–6
- Demaerel P, Baert AL, Vanopdenbosch L, Robberecht W, Dom R. Diffusion-weighted magnetic resonance imaging in Creutzfeldt-Jakob disease. *Lancet* 1997;349:847–848
- Murata T, Shiga Y, Higano S, Takahashi S, Mugikura S. Conspicuity and evolution of lesions in Creutzfeldt-Jakob disease at diffusion-weighted imaging. *AJNR Am J Neuroradiol* 2002;23:1164–1172
- Bahn MM, Parchi P. Abnormal diffusion-weighted magnetic resonance images in Creutzfeldt-Jakob disease. *Arch Neurol* 1999;56:577–583
- Schwaninger M, Winter R, Hacke W, et al. Magnetic resonance imaging in Creutzfeldt-Jakob disease: evidence of focal involvement of the cortex. *J Neurol Neurosurg Psychiatry* 1997;63:408–409
- Geschwind M, Martindale J, Young G, et al. FLAIR and diffusion-weighted imaging in neuropathology-confirmed Creutzfeldt-Jakob disease. Presented at: American Academy of Neurology 54th Annual Meeting, Denver, CO, April 13–20, 2002
- Schröter A, Zerr I, Henkel K, Tschampa HJ, Finkenstaedt M, Poser S. Magnetic resonance imaging in the clinical diagnosis of Creutzfeldt-Jakob disease. *Arch Neurol* 2000;57:1751–1757
- Shiga Y, Miyazawa K, Sato S, et al. Diffusion-weighted MRI abnormalities as an early diagnostic marker for Creutzfeldt-Jakob disease. *Neurology* 2004;63:443–449
- Kretschmar HA, Ironside JW, DeArmond SJ, Tateishi J. Diagnostic criteria for sporadic Creutzfeldt-Jakob disease. *Arch Neurol* 1996;53:913–920
- Masters CL, Harris JO, Gajdusek DC, Gibbs CJ Jr, Bernoulli C, Asher DM. Creutzfeldt-Jakob disease: patterns of worldwide occurrence and the significance of familial and sporadic clustering. *Ann Neurol* 1979;5:177–188
- Deliganis AV, Fisher DJ, Lam AM, Maravilla KR. Cerebrospinal fluid signal intensity increase on FLAIR MR images in patients under general anesthesia: the role of supplemental O₂. *Radiology* 2001;218:152–156
- Wong ST, Hoo KS Jr, Knowlton RC, et al. Design and applications of a multimodality image data warehouse framework. *J Am Med Inform Assoc* 2002;9:239–254
- Georgiades CS, Itoh R, Golay X, van Zijl PC, Melhem ER. MR imaging of the human brain at 1.5 T: regional variations in transverse relaxation rates in the cerebral cortex. *AJNR Am J Neuroradiol* 2001;22:1732–1737
- Diggle PJ, Liang KY, Zeger SL. *Analysis of Longitudinal Data*. Oxford University Press; Oxford, U.K.:1994
- Fleiss J, Cohen J, Everitt B. Large-sample standard errors of kappa and weighted kappa. *Psychological Bulletin* 1969;72:323–327
- Kropp S, Finkenstaedt M, Zerr I, Schröter A, Poser S. Diffusion-

- weighted MRI in patients with Creutzfeldt-Jakob disease. *Nervenarzt* 2000;71:91-95
30. Zeidler M, Will RG, Ironside JW, Sellar R, Wardlaw J. Creutzfeldt-Jakob disease and bovine spongiform encephalopathy: magnetic resonance imaging is not a sensitive test for Creutzfeldt-Jakob disease. *BMJ* 1996;312:844
 31. Vrancken AF, Frijns CJ, Ramos LM. FLAIR MRI in sporadic Creutzfeldt-Jakob disease. *Neurology* 2000;55:147-148
 32. Zeidler M, Collie DA, Macleod MA, Sellar RJ, Knight R. FLAIR MRI in sporadic Creutzfeldt-Jakob disease. *Neurology* 2001;56:282
 33. Mendez OE, Shang J, Jungreis CA, Kaufner DI. Diffusion-weighted MRI in Creutzfeldt-Jakob disease: a better diagnostic marker than CSF protein 14-3-3? *J Neuroimaging* 2003;13:147-151
 34. Demaerel P, Heiner L, Robberecht W, Sciot R, Wilms G. Diffusion-weighted MRI in sporadic Creutzfeldt-Jakob disease. *Neurology* 1999;52:205-208
 35. Barboriak DP, Provenzale JM, Boyko OB. MR diagnosis of Creutzfeldt-Jakob disease: significance of high signal intensity of the basal ganglia. *AJR Am J Roentgenol* 1994;162:137-140
 36. de Priester JA, Jansen GH, de Kruijk JR, Wilmink JT. New MRI findings in Creutzfeldt-Jakob disease: high signal in the globus pallidus on T1-weighted images. *Neuroradiology* 1999;41:265-268
 37. Na DL, Suh CK, Choi SH, et al. Diffusion-weighted magnetic resonance imaging in probable Creutzfeldt-Jakob disease: a clinical-anatomic correlation. *Arch Neurol* 1999;56:951-957
 38. Poon MA, Stuckey S, Storey E. MRI evidence of cerebellar and hippocampal involvement in Creutzfeldt-Jakob disease. *Neuroradiology* 2001;43:746-749
 39. Matsusue E, Kinoshita T, Sugihara S, Fujii S, Ogawa T, Ohama E. White matter lesions in panencephalopathic type of Creutzfeldt-Jakob disease: MR imaging and pathologic correlations. *AJNR Am J Neuroradiol* 2004;25:910-918
 40. Tzeng BC, Chen CY, Lee CC, Chen FH, Chou TY, Zimmerman RA. Rapid spongiform degeneration of the cerebrum and cerebellum in Creutzfeldt-Jakob encephalitis: serial MR findings. *AJNR Am J Neuroradiol* 1997;18:583-586
 41. Jin K, Shiga Y, Shibuya S, et al. Clinical features of Creutzfeldt-Jakob disease with V180I mutation. *Neurology* 2004;62:502-505
 42. Nitrini R, Mendonca RA, Huang N, LeBlanc A, Livramento JA, Marie SK. Diffusion-weighted MRI in two cases of familial Creutzfeldt-Jakob disease. *J Neurol Sci* 2001;184:163-167
 43. Collie DA, Summers DM, Sellar RJ, et al. Diagnosing variant Creutzfeldt-Jakob disease with the pulvinar sign: MR imaging findings in 86 neuropathologically confirmed cases. *AJNR Am J Neuroradiol* 2003;24:1560-1569
 44. Molloy S, O'Laoide R, Brett F, Farrell M. The "Pulvinar" sign in variant Creutzfeldt-Jakob disease. *AJR Am J Roentgenol* 2000;175:555-556
 45. Petzold GC, Westner I, Bohner G, Einhaupl KM, Kretzschmar HA, Valdueza JM. False-positive pulvinar sign on MRI in sporadic Creutzfeldt-Jakob disease. *Neurology* 2004;62:1235-1236
 46. Kropp S, Schulz-Schaeffer WJ, Finkenstaedt M, et al. The Heidenhain variant of Creutzfeldt-Jakob disease. *Arch Neurol* 1999;56:55-61
 47. Sadowski M, Tang CY, Aguinaldo JG, Carp R, Meeker HC, Wisniewski T. In vivo micro magnetic resonance imaging signal changes in scrapie infected mice. *Neurosci Lett* 2003;345:1-4
 48. Bouzamondo E, Milroy AM, Ralston HJ III, Prusiner SB, DeArmond SJ. Selective neuronal vulnerability during experimental scrapie infection: insights from an ultrastructural investigation. *Brain Res* 2000;874:210-215
 49. DeArmond SJ, Sanchez H, Yehiely F, et al. Selective neuronal targeting in prion disease. *Neuron* 1997;19:1337-1348
 50. Vernino S, Tuite P, Adler CH, et al. Paraneoplastic chorea associated with CRMP-5 neuronal antibody and lung carcinoma. *Ann Neurol* 2002;51:625-630
 51. Hirai T, Korogi Y, Yoshizumi K, Shigematsu Y, Sugahara T, Takahashi M. Limbic lobe of the human brain: evaluation with turbo fluid-attenuated inversion-recovery MR imaging. *Radiology* 2000;215:470-475